Adenosine receptor 2B activity promotes autonomous growth, migration as well as vascularization of head and neck squamous cell carcinoma cells

Max Wilkat, Hanna Bast, Robert Drees, Johannes Dünser, Amelie Mahr, Ninel Azoitei, Ralf Marienfeld, Felicia Frank, Magnus Brhel, Alexey Ushmorov, Jens Greve, Eva Goldberg Bockhorn, Marie Nicole Theodoraki, Johannes Doescher, Simon Laban, Patrick J. Schuler, Thomas K. Hoffmann, Cornelia Brunner

Adenosine receptor 2B activity promotes autonomous growth, migration as well as vascularization of head and neck squamous cell carcinoma cells

Max Wilkat[1], Hanna Bast[1], Robert Drees[1], Johannes Dünser[1], Amelie Mahr[1], Ninel Azoitei[2], Ralf Marienfeld[3], Felicia Frank[1], Magnus Brhel[1], Alexey Ushmorov[4], Jens Greve[1], Eva Goldberg-Bockhorn[1], Marie-Nicole Theodoraki[1], Johannes Doescher[1], Simon Laban[1], Patrick J. Schuler[1], Thomas K. Hoffmann[1] and Cornelia Brunner [1]

[1]Department of Oto-Rhino-Laryngology, Head and Neck Surgery, Ulm University Medical Center, Ulm, Germany
[2]Department of Internal Medicine I, Ulm University Medical Center, Ulm, Germany
[3]Ulm University, Institute of Pathology, Ulm, Germany
[4]Department of Physiology Chemistry, Ulm University, Ulm, Germany

Adenosine is a signaling molecule that exerts dual effects on tumor growth: while it inhibits immune cell function and thereby prevents surveillance by the immune system, it influences tumorigenesis directly *via* activation of adenosine receptors on tumor cells at the same time. However, the adenosine-mediated mechanisms affecting oncogenic processes particularly in head and neck squamous cell carcinomas (HNSCC) are not fully understood. Here, we investigated the role of adenosine receptor activity on HNSCC-derived cell lines. Targeting the adenosine receptor A2B (ADORA2B) on these cells with the inverse agonist/antagonist PSB-603 leads to inhibition of cell proliferation, transmigration as well as VEGFA secretion *in vitro*. At the molecular level, these effects were associated with cell cycle arrest as well as the induction of the apoptotic pathway. In addition, shRNA-mediated downmodulation of ADORA2B expression caused decreased proliferation. Moreover, in *in vivo* xenograft experiments, chemical and genetic abrogation of ADORA2B activity impaired tumor growth associated with decreased tumor vascularization. Together, our findings characterize ADORA2B as a crucial player in the maintenance of HNSCC and, therefore, as a potential therapeutic target for HNSCC treatment.

What's new?

The adenosinergic system plays an important role in the development of many types of cancer. However, the underlying mechanisms remain poorly understood. This study set to identify the oncogenic function of the adenosine receptor 2B (ADORA2B) in head and neck squamous cell carcinoma (HNSCC)-derived tumor cells. The results show that ADORA2B is upregulated and constitutively active in HNSCC-derived cell lines. This activity is sufficient to promote autonomous cell growth, migration, and angiogenesis *in vitro* and *in vivo*. The data suggest ADORA2B as an important biomarker and potential therapeutic target for the treatment of HNSCC and other ADORA2B-expressing solid tumors.

Introduction

HNSCC is the sixth most common cancer entity within the male population worldwide with an incidence of about 690.000 per year (2015).[1] More than 90% of all head and neck cancers represent HNSCC, originating from different anatomic sites and caused by diverse etiological agents, for example, alcohol, tobacco, but also HPV-infection.[2] Despite increasing treatment options, HNSCC is characterized by poor prognosis with a 5-year overall survival rate of approximately 50%, often associated with loco-regional recurrence of the tumor and distant metastasis.[2] Recently, an immunosuppressive character of the HNSCC microenvironment has been revealed.[3] The purine nucleoside adenosine (ADO) was identified among the immunosuppressive factors.[4]

Inside the tumor microenvironment (TME), ADO can be produced by immune cells, stromal and endothelial cells as well as tumor cells, expressing CD39 (gene name: *ENTPD1*) and CD73 (gene name: *NT5E*) on their surface. ADO is generated by the sequential conversion of extracellular ATP or ADP to AMP and further to ADO by the ectonucleotidases ENTPD1 and NT5E, respectively.[5] ADO causes suppression of antitumor immunity due to inhibitory effects on e.g. cytotoxic CD8$^+$ cells. At the same time ADO induces the differentiation of regulatory T cells (Treg) within the TME, which further suppresses the immune system.[4,6] Moreover, recent reports indicate that exosomes, derived from tumor cells or suppressive populations inside the TME, express high levels of ENTPD1/ NT5E on their surface and are therefore able to spontaneously generate ADO,[4,7] further contributing to immunosuppression within the TME.

The TME extracellular concentration of ADO is relatively high when compared to healthy tissue.[8] ADO activates four different G-protein coupled receptors (GPCR), A1, A2A, A2B and A3.[9] Importantly, tumor cells themselves also express ectonucleotidases as well as ADO receptors. Therefore, besides its suppressive effects on immune cells, ADO directly modulates neoplastic cell activities.[6] ADO may exert opposite effects on tumor cells, pro- or anti-tumorigenic, depending on the type of ADO receptor predominantly expressed and on the tumor entity itself. Thus, intervention with an ADORA1 antagonist induces apoptosis in breast cancer and colon cancer cells.[10–12] Furthermore, the activation of ADORA2A induces apoptosis in Caco-2 human colon cancer and HepG2 hepatoma cells.[13,14] In contrast, a protumorigenic effect upon A2A receptor activation was reported in lung and breast cancer cells.[15,16] Also, by acting *via* A3 receptor in different tumor types protumorigenic and antitumorigenic effects were observed.[17–20]

In a wide range of tumor entities, including bladder urothelial carcinoma,[21,22] colon carcinoma,[23] prostate cancer,[24,25] breast cancer,[22,24,26] melanoma[24] and also in tumors of the oral cavity,[27] an A2B-mediated protumorigenic effect was observed. However, the precise role of the adenosinergic system in HNSCC remains poorly understood. In order to elucidate whether targeting of the adenosinergic system could be a future treatment option for patients suffering from HNSCC or in general from tumor entities upregulating ADORA2B expression, the present study aims to characterize the biological consequences of the expression and function of the adenosinergic axis for HNSCC cancerogenesis. For this, *in vitro* and *in vivo* studies were applied using HNSCC-derived cell lines as well as ADORA2B expressing prostate cancer cell lines, for which a link between ADORA2B activity and cell proliferation was previously suggested.[24,25]

Materials and Methods
Cell lines and cell culture

A total of 10 HNSCC cell lines were used (the study was approved by the local Ethics Committee #219/17) including UD (University of Düsseldorf; source: Henning Bier) -SCC-1 (RRID:CVCL_E324), SCC-2 (RRID:CVCL_E325), SCC-3 (RRID:CVCL_E326), SCC-5 (RRID:CVCL_L548), SCC-6 (RRID:CVCL_M120), SCC-8 (RRID:CVCL_YD74) and UM (University of Michigan; source: Thomas E. Carey) -SCC-10A (RRID:CVCL_7713), SCC-11B (RRID:CVCL_7716), SCC-17B (RRID:CVCL_7725) and SCC-22B (RRID:CVCL_7732).[28,29] HNSCC cell lines were cultured in DMEM free of pyruvate (Life Technologies, Carlsbad, CA) supplemented with 10% FBS (Biochrom, Cambridge, UK) and 1% penicillin/streptomycin (PAN Biotech GmbH, Aiden Bach, Germany) or ZellShield: Minerva (Biolabs, Ipswich, MA) at 37°C and 5% CO$_2$. For different experiments (proliferation assay, scratch assay and VEGFA-ELISA), the amount of FBS was reduced to 1% or even replaced by 0.1% BSA (PAA Laboratories, Toronto, Ontario, Canada; migration assay). The Burkitt lymphoma cell line Namalwa (RRID: CVCL_0067; source: ATCC) as well as the prostate cancer cell lines (source: ATCC) DU145 (RRID:CVCL_0105), PC-3 (RPID: CVCL_0035) and LNCaP (clone FGC; RRID:CVCL_1379) were cultured using RPMI (Life Technologies GmbH) supplemented with 10% FBS and 1% penicillin/streptomycin at 37°C and 5% CO$_2$. The acute T cell leukemia cell line Jurkat (RRID:CVCL_0065; source: ATCC) was cultured in DMEM (Life Technologies GmbH) supplemented with 10% FBS and 1% penicillin/streptomycin at 37°C and 5% CO$_2$. The identity of all cell lines was

proven by STR analyses within the last 3 years. HNSCC-derived cell lines were additionally verified by sequencing of *TP53* gene mutations.[28,29] CD19-positive B cells were isolated from human tonsils by positive selection using microbeads (Miltenyi Biotec, Bergisch Gladbach, Germany). All experiments were performed with mycoplasma-free cells.

Short hairpin RNA vector cloning and lentiviral infection

The sequence of ADORA2B shRNA (5′-ACCGG-**GCTGGT GATCTACATTAAGAT**-GTTAATATTCATAGC-**ATCTTAAT GTAGATCACCAGC**-TTTTTTg-3′; 5′-aattCAAAAAA-**GCTG GTGATCTACATTAAGAT**-GCTATGAATATTAAC-**ATCTTA ATGTAGATCACCAGC**-C-3′) was obtained from the Broad Institute GPP Web Portal TRC2 library (http://portals.broadinstitute.org/ gpp/public/clone/details?cloneId=TRCN0000065334) and was cloned into the BbsI and EcoRI sites of the pRSI12-U6-sh-UbiC-TagRFP-2A-puro vector (Cellecta; https://www.cellecta.com/), obtained from BioCat. The scrambled shRNA was described elsewhere.[30] shRNA were overexpressed using the lentiviral pRSI12-U6-sh-UbiC-TagRFP-2A-puro vector. The production of lentiviral particles was described.[30] HNSCC cell line was transduced by co-cultivation with 430 μl lentiviral particles in the presence 570 μl GibcoOpti-MEM I reduced serum medium, no phenol red, and 8 μg/ml polybrene. Cells were incubated at 37°C for 72 hr. Then, viral supernatant was removed and DMEM (high glucose, no pyruvate, 10% FBS and 1% PenStrep) was added. After 48 hr, the puromoycin selection was started (1.5 to 5 μg/ml, until cells were 100% RFP positive).

RNA isolation and cDNA synthesis

RNA was prepared using the QIAzol Lysis Reagent (Qiagen) in combination with a SubQ syringe (Becton Dickinson, San Diego, CA). Reverse transcription was performed using random hexamer primers (0.2 μg/μl; Promega, Madison, WI), 10 mM dNTPs (GE Healthcare, Chicago, IL) and AMV reverse transcriptase (10 U/μl; New England Biolabs, Ipswich, MA).

Detection of *ADORA*-transcripts

The transcripts of *ADORA1*, *ADORA2A*, *ADORA2B*, *ADORA3* and *GAPDH* were amplified by end point-PCR from tumor cells and positive control samples (*ADORA1*: CD19-positive B-cells isolated from human tonsil tissue; *ADORA2A*: Jurkat T cells; *ADORA2B*: prostate cancer cell lines; *ADORA3*: Glioblastoma) using specific primers[25] (Supporting Information Table S1). Products were separated on 1.8% agarose gels and visualized by Midori Green Advance DNA Stain (NIPPON GENETICS EUROPE GmbH) using the ChemiDoc MP Imaging System (Bio-Rad Laboratories GmbH, Munich, Germany). Three independent experiments were performed.

Quantitative expression analysis of *ADORA2B*, *ENTPD1* and *NT5E*

Relative mRNA expression was quantified by SYBR Green PCR assay. Specific primers (Supporting Information Table S2) were obtained from biomers.net GmbH. Gene-specific PCR products were measured with the LightCycler 96 Instrument (Hoffmann-La Roche AG). For relative quantification the $2^{-\Delta\Delta CT}$-method was used.[31]

Detection and quantification of ENTPD1 and NT5E on cell surfaces

Cells were stained using monoclonal anti-CD39PE-Cyanine seven coupled antibodies, eFluor 450 coupled anti-CD73-antibodies and corresponding murine IgG1 kappa isotype control antibodies (eBioscience, San Diego, CA). Flow cytometry was performed using a Gallios Flow Cytometer (Beckmann Coulter Life Sciences, San Jose, CA). The mean fluorescence intensity was determined.

Western blotting

Western blots were performed according standard procedures using 3–20 μg of total protein extracts. Membranes were stained with anti-ADORA2B (Abcam), cyclin-D1 (CCND1), pRB1 (Ser780), Bcl-xl (BCL2L1), caspase 9 (CASP9), LC3A/B (MAP1LC3A/B) and ATG7 antibodies (all obtained from Cell Signaling) and anti-β-actin (AKTB) monoclonal mouse antibody (Sigma-Aldrich, St. Louis, MO). The secondary antibodies were received from Thermo-Scientific. For densitometry analyses, the ChemiDoc™ MP imaging system (Bio-Rad) as well as Image Lab Version 5.2.1 software (Bio-Rad) were used.

Proliferation assay

Cell proliferation was assessed by MTT assay using the CellTiter 96 nonradioactive cell proliferation assay (Promega Corporation, Fitchberg, WI). Then, 1×10^3 cells per well were seeded on 96-well plates and grown at 37°C and 5% CO_2 in complete DMEM (10% FBS). After 24 hr, fresh medium was given (1% FBS) containing DMSO or PSB-603 (1–10 μM; Sigma Aldrich). The absorbance was measured with a Tecan Infinite M200 Pro microplate reader (Tecan Group AG). Three experiments were performed in quadruples. The proliferative capacity of shRNA-expressing cells was assessed by the xCELLigence real time cell analysis system (OMNI Life Science). Electrodes were coated with 1% fibronectin for 30 min at RT and 5×10^3 cells/well were seeded in triplicates in complete DMEM (10% FBS). Proliferation was monitored over time.

Scratch assay/wound closure assay

A total of 3×10^4 cells per cm^2 were seeded on 12-well plates in DMEM supplemented with 10% FBS and cultivated at 37°C and 5% CO_2 overnight. An artificial wound was scratched into the confluent cell monolayer using a pipette tip of a 1,000 μl pipette. Photomicrograph images (Axio Observer D1 fluorescence microscopy, Carl Zeiss AG) were immediately captured (time 0 hr), and the cells were subsequently incubated in

DMEM (1% FBS) supplemented with DMSO, NECA, NECA +PSB or PSB (each 1 μM; Sigma Aldrich). In case of co-incubation (NECA+PSB), PSB was added 20 min after NECA. The migration of the cells and the closing of the scratch were observed by taking microphotographs. Three experiments were performed in triplicate.

Migration assay

Two-chamber migration apparatus (pore size 8 μm) was used (Falcon Corning Inc, Corning, NY) to perform cell migration assays. Then, 1×10^6 cells were seeded in the upper chamber in serum free medium supplemented with 0.1% BSA. Medium supplemented with 10% FBS was added to the lower chamber as the chemoattractant. In both chambers DMSO, NECA, NECA+PSB-603 or PSB-603 (each 1 μM) were added. In case of co-incubation (NECA+PSB-603), PSB-603 was added 20 min after NECA. After 16 hr incubation at 37°C and 5% CO_2, cells were carefully removed from the upper chamber using a cotton swab and the cells that had traversed the membrane were fixed with 3.7% paraformaldehyde and stained with DAPI. Cells fluorescence was monitored with an Axio Observer D1 microscope (Carl Zeiss AG). Images were captured using the software Axio Vision 40 (Carl Zeiss Imaging Solutions GmbH). The cell nuclei in the captured images were counted for each experimental condition. Three experiments were performed in duplicate.

VEGFA-ELISA

HNSCCs were seeded with a density of 2.5×10^4 cells per cm^2 on 12-well plates and grown at 37°C and 5% CO_2 in complete DMEM (10% FBS) overnight. Medium was replaced (0 hr time) with DMEM (1% FBS) supplemented with either DMSO or PSB-603 (1 μM). Supernatants were collected and subjected to detection of VEGFA release using a human VEGFA ELISA Kit (Life Technologies) following the manufacturer instruction manual. Extinction was analyzed at 450 nm using Infinite M200 Pro microplate reader (Tecan Group AG) and Magellan V7.1 software (Tecan Group AG). The experiment was performed three times in duplicate.

cAMP measurement

Intracellular cAMP levels were determined using the cAMP parameter assay kit from R&D systems according to the manufacturer's instructions using Infinite M200 Pro microplate reader (Tecan Group AG) and Magellan V7.1 software (Tecan Group AG).

Cell-cycle analysis and apoptosis assays

Cell cycle analysis was performed as described earlier.[25] Flow cytometry analyses of Annexin V (Abcam) and 7AAD (BD Biosciences) were performed to examine apoptosis. Additionally, the TUNEL-Assay-Kit-FITC (Abcam) was applied according to the manufacturer's instructions.

Chorionallantoic membrane assay and IHC analysis

Chorionallantoic membrane (CAM) assays were performed as described.[32] Briefly, 1.5 or 2.0 × 10^6 cancer cells as indicated were applied within 5 mm silicon rings on the surface of the chicken CAM, 8 days after egg fertilization. Xenografts were either treated with vehicle control or treated with different concentrations of the ADORA2B inverse agonist/antagonist PSB-603 (1, 2.5 or 5 μM) 24 and 48 hr after tumor xenograft. Four days after implantation tumors were harvested and photographed. Tumor area was quantified using ImageJ software.[33] Tumors were fixed in formalin, paraffin embedded and further subjected to IHC. The 5-μm sections were analyzed for pan-cytokeratin (pan-KRT; 1:1; EMD Millipore Corp.; clone AE1/AE3), desmin (DES; 1:150; Dako; clone D33) and Ki-67 (MKI67) 1:50 or 1:75; Santa Cruz; clone MIB-1). To determine the number of Ki-67-positive cells, at least 300 cells in three distinct, randomly chosen areas within the tumor (according the cytokeratin staining) were examined. Desmin reactivity was quantified by subtracting background staining from the specific desmin staining using ImageJ software.[33]

Statistical analysis

Data are expressed as the mean ± standard deviation (SD). Between groups, statistical differences were evaluated with Student's *t*-test. Statistical significance was marked with * for $p < 0.05$, ** for $p < 0.01$ and *** for $p < 0.005$.

Data availability

The data that support the findings of our study are available from the corresponding author upon reasonable request.

Results

Human HNSCC cell line express CD73 (NT5E) and ADORA2B constitutively on their surface

To analyze the presence of players of the adenosinergic system in HNSCC cells, quantitative RT-PCR (Supporting Information Fig. S1a; Fig. 1a) and flow cytometry analyses (Supporting Information Fig. S1b and S1c) detecting *ENTPD1* and *NT5E* were performed involving 10 human HNSCC-derived cell lines. As internal controls, three ADORA2B-expressing prostate carcinoma cell lines (DU145, PC-3, LnCap)[25] as well as human lymph node derived CD19$^+$ B cells, expressing ENTPD1 and NT5E but not ADORA2B at their surface,[34] were included into the study. Additionally, the Burkitt lymphoma cell line Namalwa was analyzed. While we detected a substantial expression of *ENTPD1* on CD19+ B cells, we were unable to identify any *ENTPD1* mRNA expression in prostate cancer cell lines, HNSCC cell lines or Namalwa B cells (Supporting Information Fig. S1a). In contrast, we observed a considerable expression of *NT5E* in all HNSCC-derived cell lines as well as in the analyzed prostate cancer cells. Interestingly, *NT5E* showed higher expression in cancer cells as compared to purified CD19+ B cells (Fig. 1a). The absence of ENTPD1 and the presence of NT5E expression at protein level was confirmed by flow cytometry (Supporting Information Fig. S1b and S2c). To define the

Molecular Cancer Biology
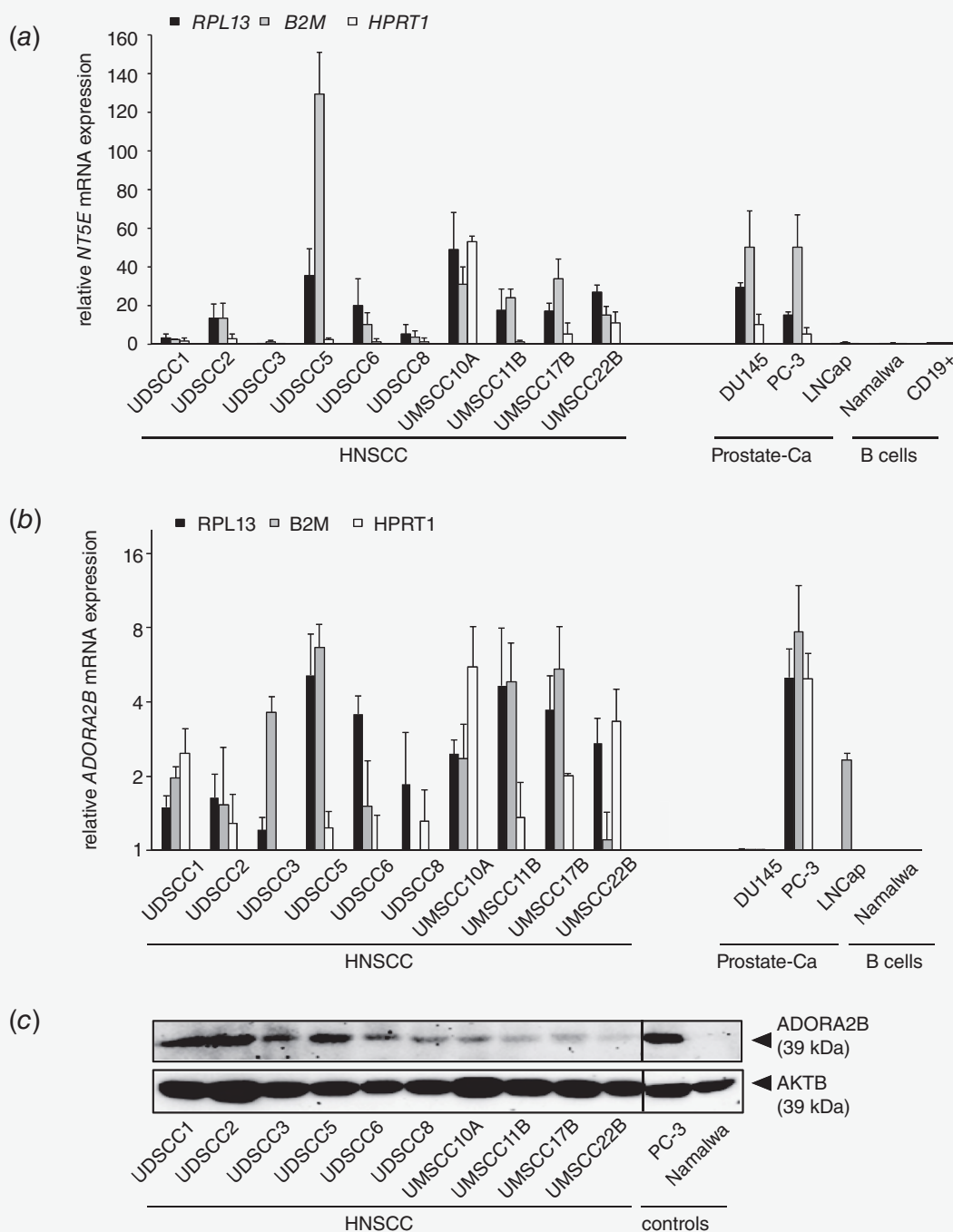
Figure 1. Ectonucleotidase *NT5E* (CD73) as well as *ADORA2B* are constitutively expressed in HNSCC-derived cell lines. (*a*) Quantitative RT-PCR analyses of *NT5E* mRNA expression in 10 HNSCC-derived cell lines relative to three different housekeeping genes (*RPL13*, *B2M*, *HPRT1*). In parallel, three prostate-carcinoma (Ca) cell lines (DU145, PC-3 and LNCap) were included into the analyses. Additionally, the Burkitt lymphoma cell line Namalwa as well as CD19+ tonsillar B cells were analyzed. *NT5E* mRNA expression levels of tumor cell lines are depicted relative to the *NT5E* transcript level of CD19 + B cells. (*b*) Quantitative RT-PCR analyses of *ADORA2B* mRNA expression in 10 HNSCC-derived cell lines relative to three different housekeeping genes (*RPL13*, *B2M*, *HPRT1*). In parallel, three prostate-carcinoma (Ca) cell lines (DU145, PC-3 and LNCap) were included into the analyses, also, the Burkitt lymphoma cell line Namalwa as well as CD19+ tonsillar B cells. *ADORA2B* mRNA expression levels of tumor cell lines are depicted relative to the *ADORA2B* transcript level of the DU145 prostate-carcinoma (Ca) cell line, for which *ADORA2B* expression was described previously.[25] (*a* and *b*) Each individual experiment was performed in duplicates. Three independent experiments were performed. Presented are the mean values ± SD. (*c*) Evaluation of ADORA2B protein expression by Western Blotting. The detection of AKTB (β-Actin) served as loading control.

exact ADO-sensing receptors expressed in HNSCC cell lines, endpoint RT-PCR experiments were performed. These revealed that all analyzed HNSCC cell lines expressed exclusively *ADORA2B* (Supporting Information Fig. S2). In line with published data,[25] prostate cancer cell lines DU145, PC-3 and LnCap also express ADORA2B, with the highest expression detected in PC-3 cells. In contrast, expression of A1, A2A and A3 receptors was not observed in any of the analyzed HNSCC, prostate carcinoma or Burkitt lymphoma cell lines (Supporting Information Fig. S2). The expression of *ADORA2B* was further evaluated by quantitative RT-PCR. To exclude a potential deregulation of housekeeping genes, three different genes, *RPL13*, *B2M* and *HPRT1*, were used for normalization, resulting in different ADORA2B expression levels estimations (Fig. 1*b*). Immunoblotting analysis confirmed ADORA2B expression (Fig. 1*c*) in all HNSCC cell lines tested, albeit at different extent.

ADORA2B activity affects proliferation, migration and VEGFA secretion of HNSCC cells

To characterize the oncogenic potential of ADORA2B activity on HNSCC, cells were treated with different concentrations of ADO and monitored over time. Surprisingly, we did not observe any effect on cell proliferation induced by ADO (Fig. 2*a*). Only the use of high concentrations of ADO (10 mM) was associated with reduced proliferation. However, this observation was rather due to an ADORA2B-independent, toxic effect, since proliferation of Namalwa cells, which do not express ADORA2B or any other ADO receptor, was also affected at this high ADO concentrations (Figs. 1*b* and 1*c* and Supporting Information Fig. S2). This hypothesis was confirmed by AnnexinV/7AAD staining as well as by TUNEL assays, revealing a significant increase of apoptotic cells upon treatment with 10 mM ADO (Supporting Information Figs. S3*a* and S3*b*). In contrast, the use of increasing concentrations of ADORA2B inverse agonist/antagonist PSB-603 (below just called ADORA2B antagonist) resulted in a clear concentration- and time-dependent decrease in proliferation for all HNSCC cell lines analyzed (Fig. 2*b*). Internal controls were performed with ADORA2B expressing PC-3 cells ([25] and Figs. 1*b* and 1*c*) and ADORA2B negative Namalwa cells (Figs. 1*b* and 1*c*). Of note, ADORA2B-negative Namalwa cell proliferation remained unaffected by PSB-603 treatment ranging between 1 and 5 μM. However, at concentrations of 10 μM PSB-603 Namalwa cell proliferation was severely diminished (Fig. 2*b*) suggesting an ADORA2B-independent, direct toxic effect of PSB-603. In order to exclude ADORA2B-independent PSB-603 effects, a 10 μM PSB-603 concentration was no longer used in subsequent experiments. We further confirmed the PSB-603-mediated inhibitory effect on HNSCC cell proliferation in scratch assays, in which PSB-603 significantly delayed wound closure (Figs. 2*c* and 2*d*). In contrast, for some (UDSCC1, 3, 5 and PC-3) but not all tested cell lines we observed a faster wound closure when cells were cultured in the presence of the nonselective ADORA2B agonist NECA (Figs. 2*c* and 2*d*). Interestingly, co-incubation of cancer cells with NECA together with

PSB-603 abrogated the positive effect of NECA (Figs. 2*c* and 2*d*). Together, these results indicate that HNSCC cell proliferation depends on ADORA2B activity.

To investigate which ADORA2B-mediated signaling pathways are involved in the regulation of proliferation, inhibitor studies were conducted. Similar to PSB-603 treatment, we observed a concentration-dependent inhibition of HNSCC-derived cell line proliferation when the adenylate cyclase inhibitor MDL12330A was involved, leading to comparable reduced cAMP levels as observed with PSB-603 (Figs. 2*e* and 2*f*). Therefore, our data suggest an involvement of Gα$_s$ coupled proteins responsible for elevated cAMP levels associated with ADORA2B-dependent proliferation of HNSCC.

ADORA2B expression is associated with progression of oral cavity tumors[27] and also with increased invasiveness and metastasis of triple negative breast cancer.[24] Since increased migratory activity is a prerequisite for invasiveness and metastasis, we next analyzed whether migration of HNSCC-derived cell lines depends on ADORA2B activity. We observed a substantial migratory capability of analyzed HNSCC as well as prostate cancer cell lines, which was found significantly reduced in the presence of PSB-603 in all analyzed ADORA2B-expressing cancer cells (Fig. 2*g*). Of note, treatment with NECA did not significantly increase migration of tested cell lines.

Since VEGFA is a key molecule involved in the induction of tumor vascularization, we tested whether ADORA2B activity is also necessary for VEGFA secretion by HNSCC cells. Abrogation of ADORA2B activity resulted in significant decrease in VEGFA secretion by HNSCC and prostate cancer cells (Fig. 2*h*). Interestingly, VEGFA secretion was also detectable in ADORA2B-negative Namalwa B cells, which was consequently unaffected by PSB-603 treatment. Similar to our wound closure experiments, both NECA and ADO treatments increased slightly but significantly the VEGFA secretion at concentration of 5 μM after 96 hr of treatment (Fig. 2*i*). Again, the NECA induced VEGFA secretion was suppressed by PSB-603. In addition, the phospholipase C inhibitor U73122 was also able to inhibit VEGFA secretion by HNSCC cells (Fig. 2*j*), indicating a link of ADORA2B to the Gα$_q$ subunit.

ADORA2B is constitutively active in HNSCC cells

Since ADO itself had no effect on HNSCC cell proliferation that in turn was efficiently inhibited using PSB-603, we wondered whether ADORA2B is constitutively active in HNSCC. Indeed, HNSCC cell lines UDSCC1 and UDSCC6 showed considerable high basal levels of cAMP (13–14 pmol/ml per 6×10^4 cells initially seeded). This was significantly decreased after treatment of cells with PSB-603 (Figs. 2*f*, 2*k* and 2*l*). Notably, neither ADO nor NECA treatment (2.5 and 5 μM) significantly increased intracellular cAMP levels. In line with previous reports,[35] only high concentrations of ADO (10 μM) promotes a further increase of cAMP levels in HNSCC cell lines taken into the study (Supporting Information Figs. S4*a* and S4*b*). Together with the fact that incubation of HNSCC

and PC-3 cancer cells with ADO did not result in increased proliferation (Fig. 2a), our data suggest that the constitutive and ligand-independent activity of ADORA2B promotes the autonomous proliferation, migration and VEGFA secretion of tumors of the head and neck region. Still, we could not exclude a preactivation of ADORA2B by endogenous ADO.

To evaluate this possibility, we repeated our experiments in the presence of ADO deaminase (ADA) that catabolizes ADO to Inosine. ADA did not influence basal nor NECA-induced cAMP production (Figs. 2k and 2l) indicating that in our experimental setup an influence of endogenous ADO on ADORA2B activity can be excluded.
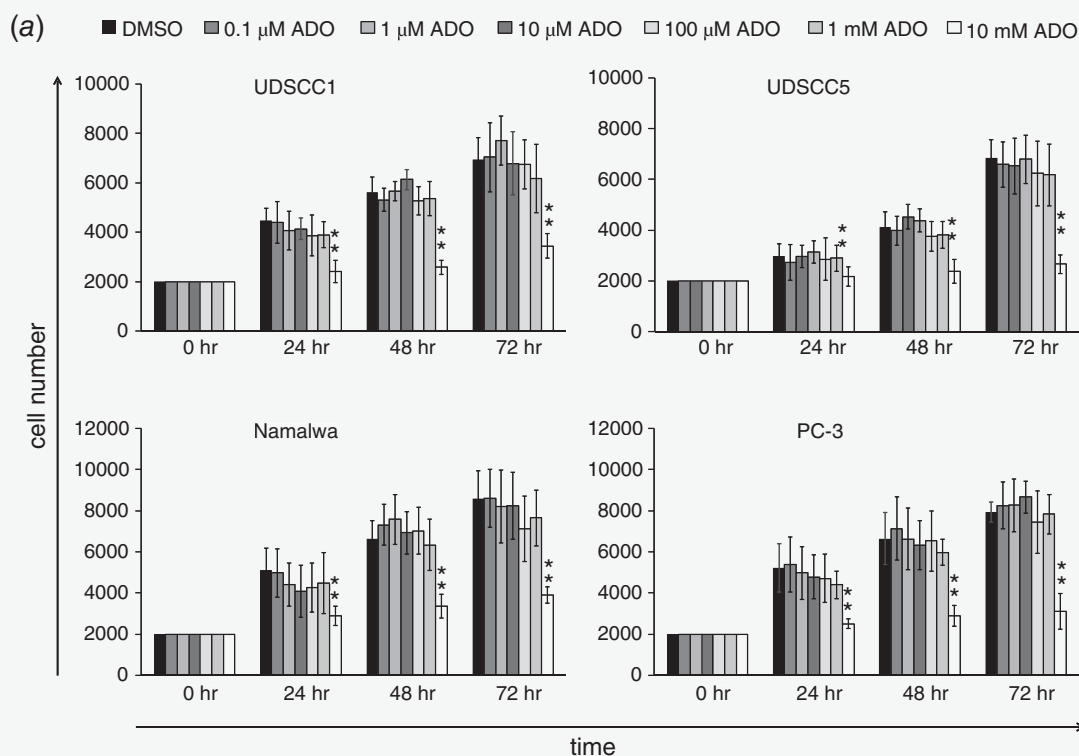
Figure 2. Constitutive ADORA2B activity drives autonomous proliferation, migration as well as VEGFA secretion of HNSCC-derived cells lines. (a) Adenosine does not induce proliferation of HNSCC-derived cell lines. Cell lines as indicated were seeded, treated with different amounts of adenosine (ADO) and proliferation was assessed over a time period of 72 hr. (b) HNSCC-derived cell lines as indicated as well as the prostate-ca cell line PC-3 (highly expressing ADORA2B; positive control) and the B lymphoma cell line Namalwa (not expressing ADORA2B; negative control) were seeded and treated with different amounts of the ADORA2B antagonist PSB-603. The proliferation was assessed over time. (c) Wound closure capacities were analyzed for HNSCC-derived cell lines as well as for the prostate-ca cell line PC-3, which were either left untreated or treated with the NECA, with the PSB-603 or with a combination of both. Wound closure was monitored microscopically (exemplary depicted for UDSCC5) and (d) evaluated taking the measurements of microphotograph images. (e, f) UDSCC1 and UDSCC6 cells were seeded and either left untreated or cultivated in the presence of PSB-603 or different concentration of the adenylate cyclase inhibitor MDL12330A. Proliferation (e) as well as intracellular cAMP levels (f) were assessed. (g) In transwell assays, the migratory capabilities of HNSCC-derived cell lines as well as of the prostate-ca cell line PC-3 were assessed in the presence of NECA, PSB-603 or in the presence of both. The percentage of migration relative to the DMSO-treated cells (control) is depicted. (h) Cell lines UDSCC1, UDSCC5, PC-3 and Namalwa were either left untreated or treated with PSB-603. After time points indicated the supernatant was taken and analyzed for the amount of secreted VEGFA. (i) UDSCC5 cells were either left untreated or treated with PSB-603, NECA, with equimolar concentrations of both compounds together or with ADO. After time points indicated the supernatant was taken and analyzed for the amount of secreted VEGFA. (j) UDSCC5 cells were either left untreated or treated with the ADORA2B antagonist PSB-603 or increasing concentrations of the phospholipase C inhibitor U73122. After time points indicated the supernatant was taken and analyzed for the amount of secreted VEGFA. (k and l) The UDSCC1 and UDSCC6 cells were either left untreated or treated with the PSB-603, NECA, with equimolar concentrations of both compounds together or with ADO at concentrations indicated, either in the absence or presence of 1 U/ml ADA. The changes in intracellular cAMP concentrations are depicted relative to the determined basal cAMP level, which was set as 1. Each individual experiment was performed in triplicates. None less than three independent experiments were performed. Presented are the mean values ± SD. Significant levels were determined relative to the DMSO control values. *p < 0.05, **p < 0.01, ***p < 0.005. Significant levels were also determined relative to samples that were treated with NECA together with PSB-603 (NECA+PSB): ##p < 0.01. [Color figure can be viewed at wileyonlinelibrary.com]
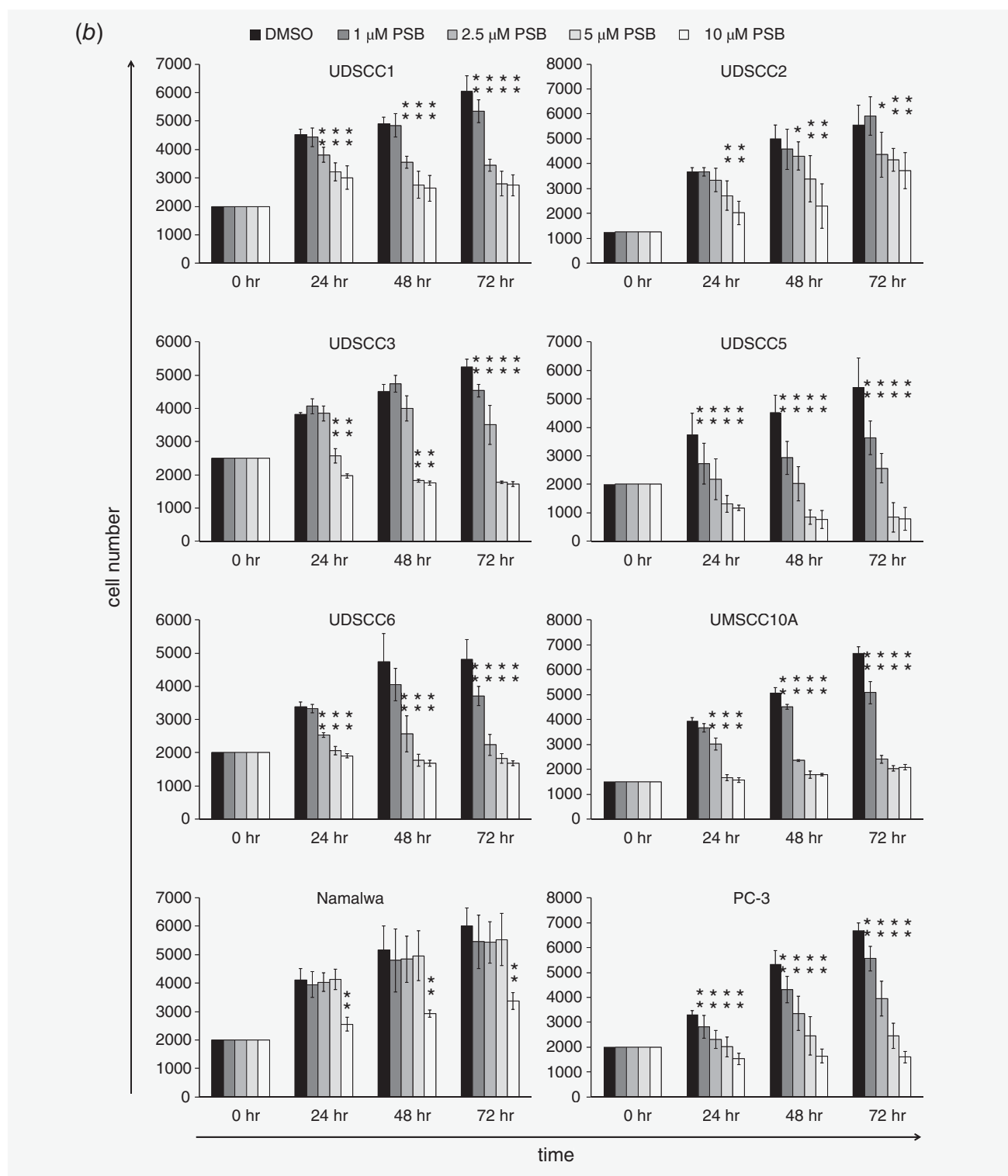
Figure 2. (Continued)

PSB-603 induces cell cycle arrest and apoptosis

To decipher the mechanisms by which PSB-603 inhibits HNSCC cell proliferation, cell cycle, apoptosis and autophagy were investigated. Cell cycle analyses of cancer cells cultivated in revealed a G1 arrest at the expense of S- and G2/M phases in UDSCC6 cells (Figs. 3*a* and 3*b*) or a G2/M arrest at the
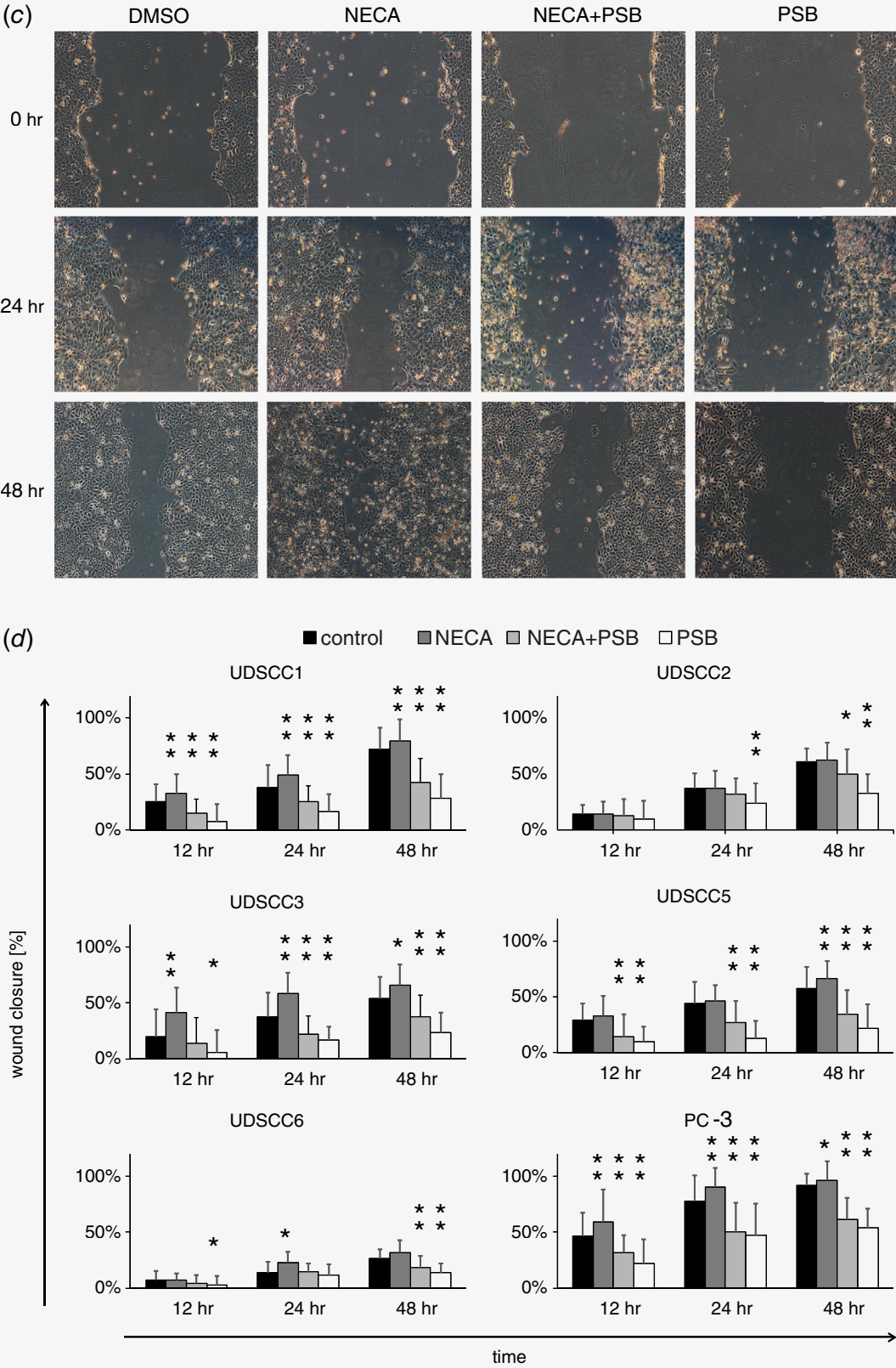
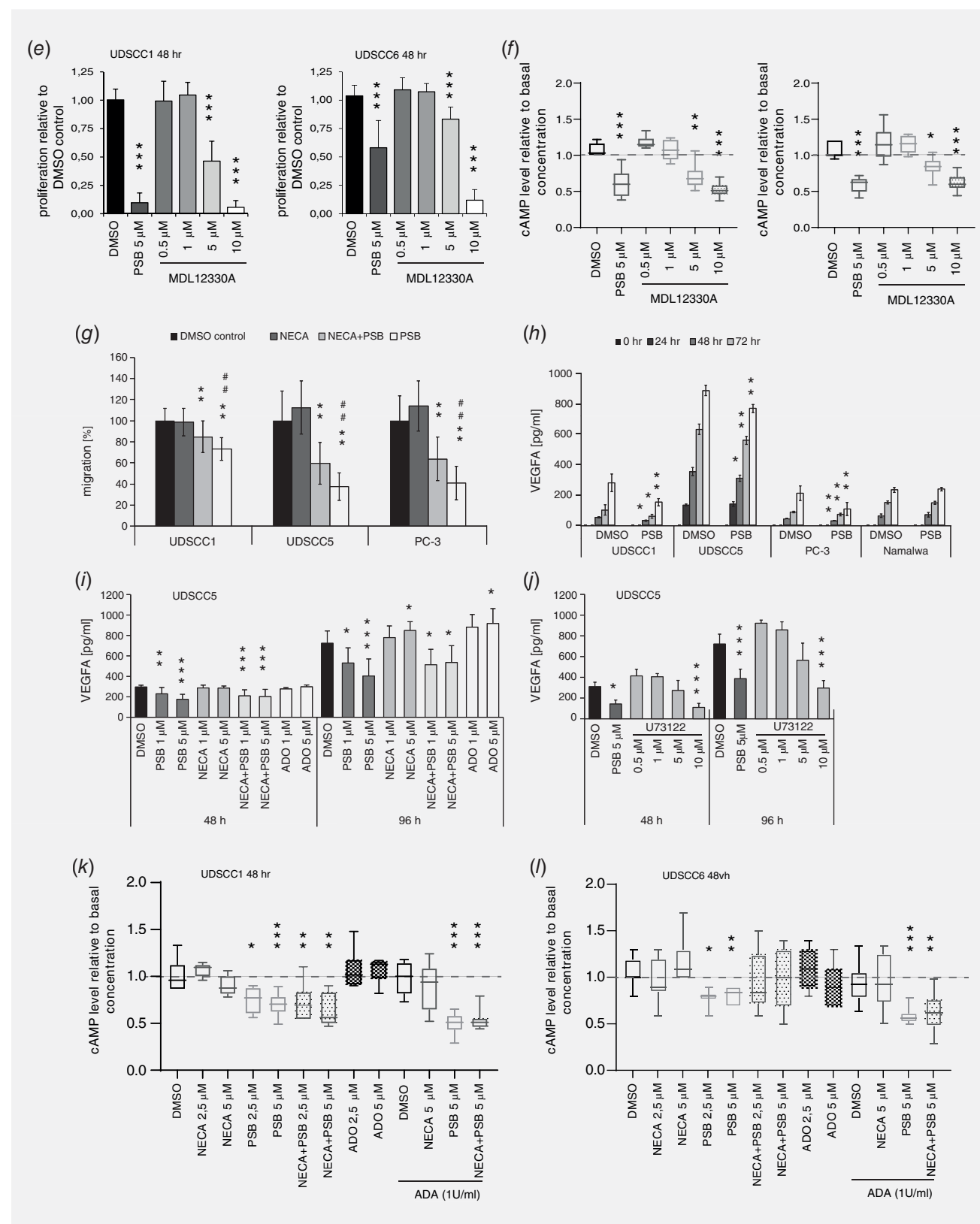Molecular Cancer Biology

Figure 2. (Continued)

Figure 2. (Continued)

expense of G0/G1 and S phase in UDSCC1 cells (Supporting Information Fig. S5) upon inhibition of ADORA2B activity. This was associated with reduced cyclin D1 (CCND1) expression as well as with impaired phosphorylation at S780 of retinoblastoma protein (RB1). At the same time, we observed a downregulation of the antiapoptotic protein Bcl-xl (BCL2L1), which was associated with enhanced levels of the proapoptotic protein cleaved caspase 9 (CASP9; Figs. 3c–3e). To corroborate these results, HNSCC cell lines were examined by Annexin V/7AAD staining as well as by TUNEL assay (Supporting Information Fig. S3). Both analyses revealed a PSB-603-induced apoptosis. Thus, in UDSCC1 and UDSCC6 cells, PSB-603 provoked cell cycle arrest and induced the programmed cell death pathway in a concentration-dependent manner (Figs. 3c–3e; Supporting Information Fig. S3). Similar to wound closure experiments, NECA has a stronger effect on UDSCC1 cell cycle progression than on

UDSCC6 cells (Supporting Information Figs. S5a–S5d and data not shown). In UDSCC1 cells, NECA promotes an increase of S-phase, most likely due to enhanced cyclin D1 and pRB1 expression. Again, NECA-induced effects were abrogated in the presence of PSB-603. In contrast, no effect of NECA on protein expression influencing cell cycle progression could be observed in UDSCC6 cells. PSB-603 treatment of cancer cells did not affect the expression of LC3A/B (MAP1LC3A/B) and ATG7 proteins, indicating no effect on autophagy (data not shown).

Inhibition of ADORA2B activity impairs tumor growth as well as angiogenesis *in vivo*

Having demonstrated the requirement of ADORA2B activity for HNSCC autonomous cell growth *in vitro*, we next analyzed the effect of ADORA2B inhibition on tumor progression
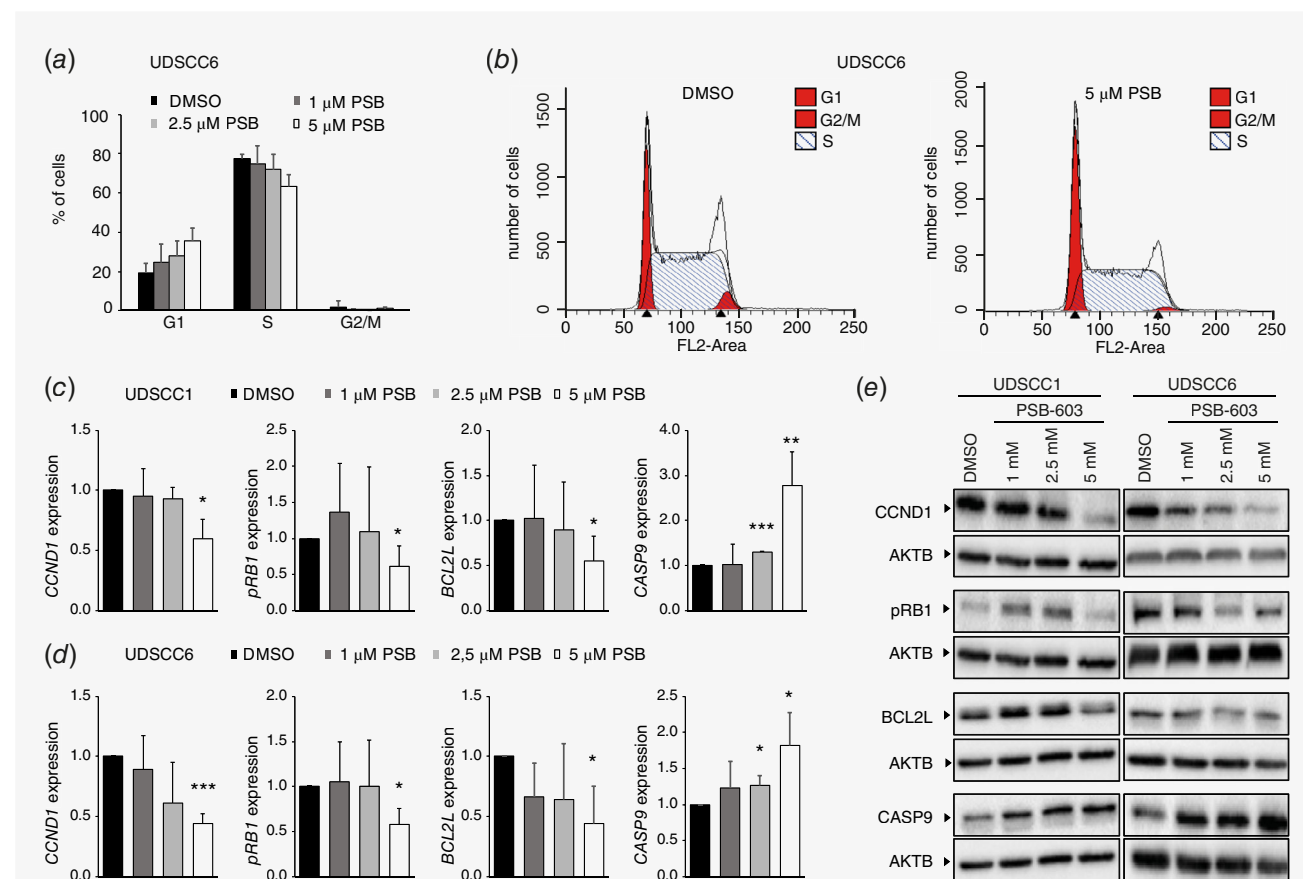
Figure 3. The ADORA2B antagonist PSB-603 stops cell cycle progression and induces the apoptotic pathway. (*a*) Cell cycle analyses were performed using UDSCC6 cells that were either left untreated (DMSO control) or were treated with PSB-603 at different concentrations as indicated for 24 hr. Depicted are the mean values ± SD of three independent experiments. (*b*) Shown are representative graphs of cell cycle analyses described in (*a*) using ModFit LT software. (*c*) UDSCC1 and (*d*) UDSCC6 cells were either left untreated (DMSO control) or treated with different concentrations of PSB-603 as indicated. After 48 hr of incubation, lysates were prepared and subjected to Western blot analysis detecting proteins involved in cell cycle regulation CCND1 and pRB1 (Ser780), or in regulation of pro- and anti-apoptotic events, cleaved CASP9 and BCL2L1. Presented are the mean values of protein expression relative to the housekeeping gene AKTB ± SD determined by densitometry analyses of three independent experiments. Bands with identical AKTB controls are derived from the same blot. Significant levels were determined relative to the DMSO control values. *$p < 0.05$, **$p < 0.01$, ***$p < 0.005$. (*e*) Representative Western blot images of experiments described in (*c*) and (*d*) are shown.
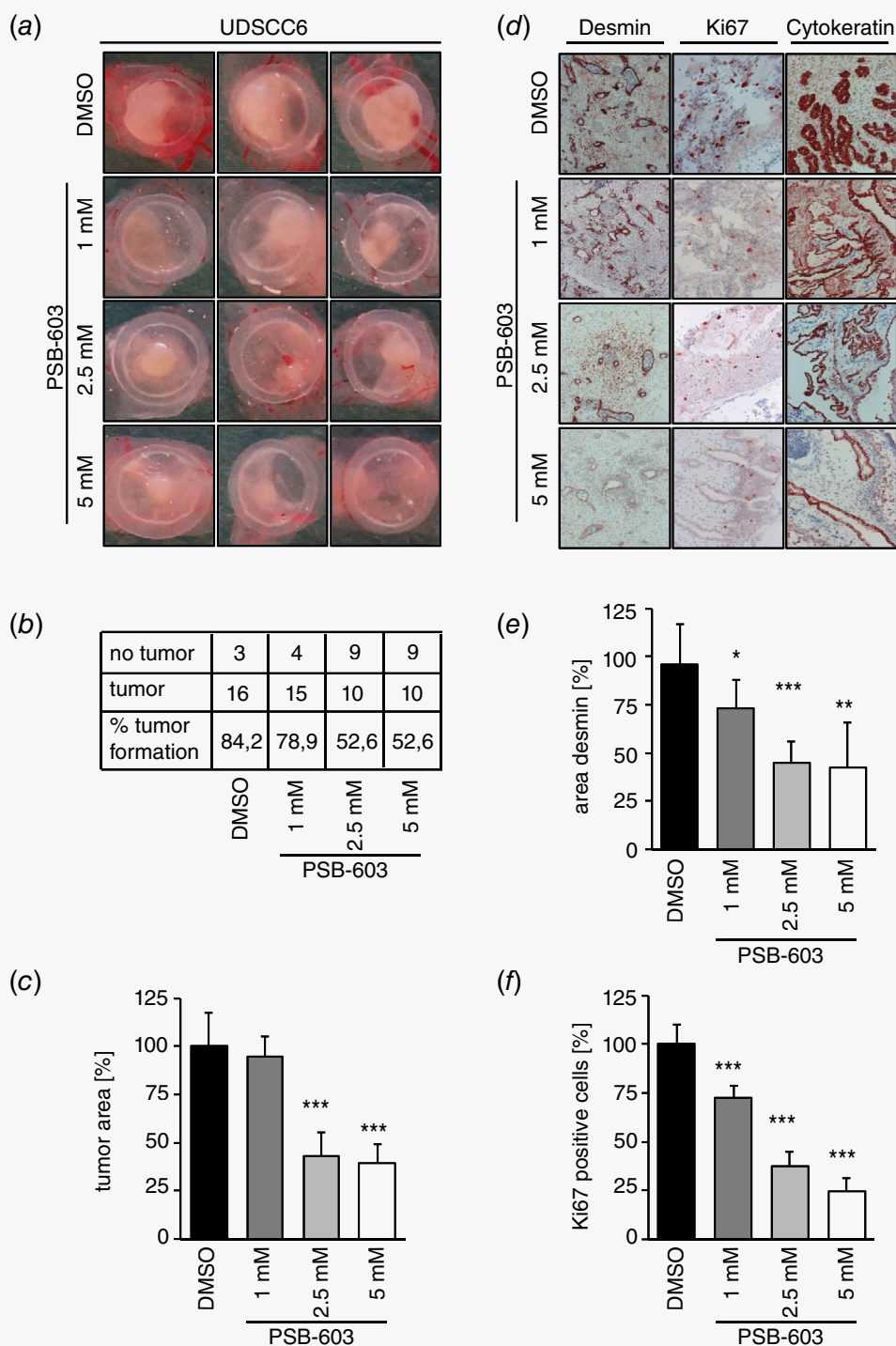
Figure 4. Inhibition of ADORA2B activity impairs tumor growth and tumor blood vessel formation on CAM. (*a*) UDSCC6 cells were applied to CAM. After 24 and 48 hr tumors were treated with concentrations as indicated of PSB-603. Four days after implantation tumors were harvested and photographed. (*b*) Evaluation of tumor formation. (*c*) Quantification of tumor area is presented. (*d*) IHC using antibodies directed against desmin (DES), Ki-67 (MKI67), and cytokeratin (pan-KRT) is depicted. (*e*) Desmin immunoreactivity was quantified by subtracting background staining from specific desmin signal using ImageJ software. (*f*) Quantification of Ki-67 positive cells is shown. Presented are the mean values $\pm$ SD. Significant levels were determined relative to the DMSO control values. *$p < 0.05$, **$p < 0.01$, ***$p < 0.005$.

Molecular Cancer Biology
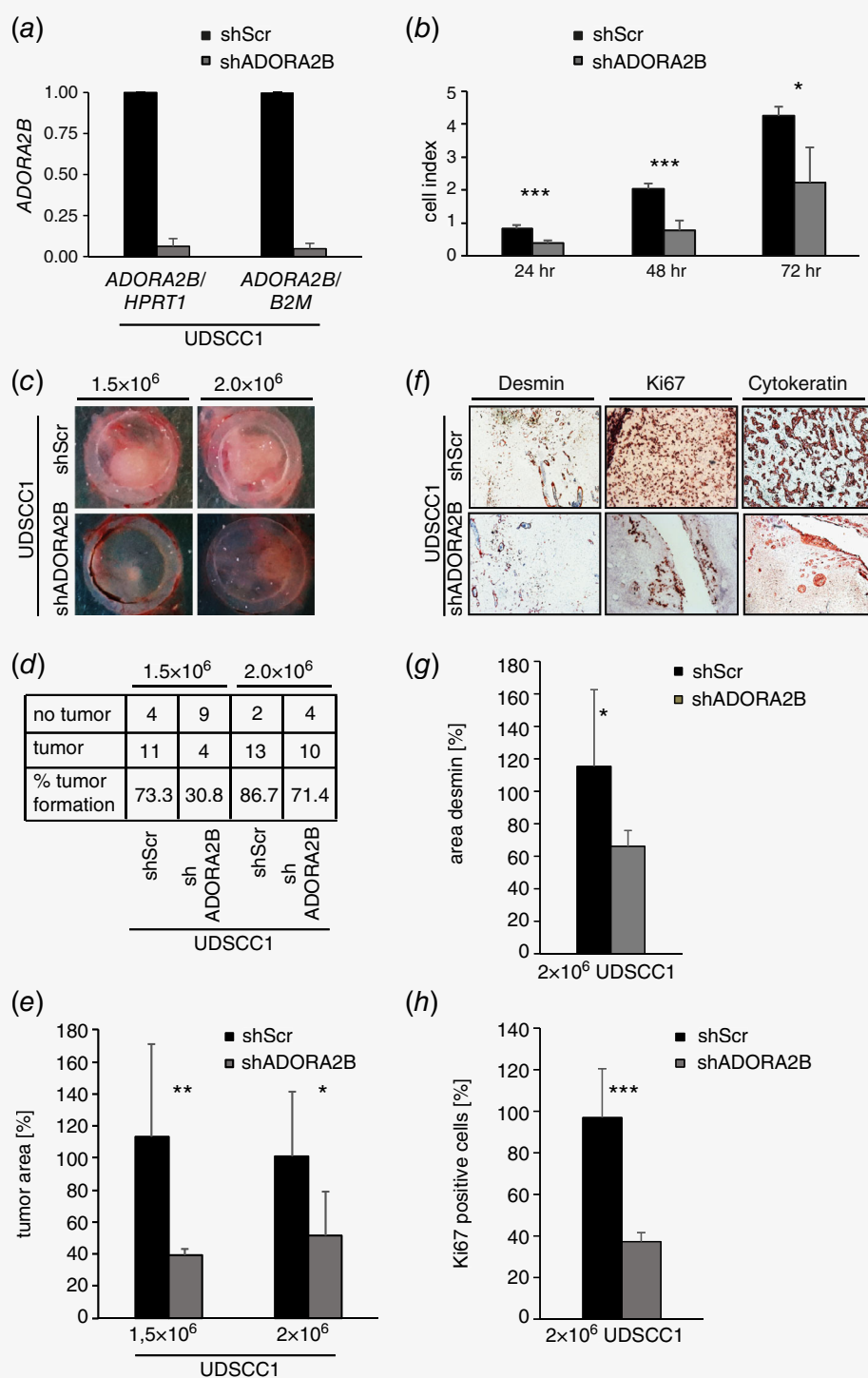
Figure 5. Down-regulation of ADORA2B expression impairs proliferation as well as tumor formation *in vitro* as well as *in vivo*. (*a*) UDSCC1 cell were lentiviral transduced with vectors expressing either scrambled (shScr) or *ADORA2B* shRNA (shADORA2B). The efficiency of *ADORA2B* down-modulation was estimated using quantitative RT-PCR by calculating *ADORA2B* expression relative to the expression determined in shScr expressing cells levels and two housekeeping genes, *HPRT1 and B2M*. (*b*) shScr or shADORA2B expressing cells were analyzed for their proliferating rates over time using a real time cell analyzer. The calculated cell index is presented mean ± SD. (*c*) shScr or shADORA2B expressing cells were applied to CAM in different amounts, either 1.5×10^6 or 2.0×10^6 cells. Four days after implantation tumors were harvested and photographs were taken. (*d*) Evaluation of tumor formation. (*e*) Quantification of tumor area is presented. (*f*) IHC using antibodies directed against desmin (DES), Ki-67 (MK67), and cytokeratin (KRT) is depicted. (*g*) Desmin immunoreactivity was quantified by subtracting background staining from specific desmin signal using ImageJ software. (*h*) Quantification of Ki-67 positive cells is shown. Presented are the mean values ± SD. *p < 0.05, **p < 0.01, ***p < 0.005.

in vivo using the chicken chorioallantoic membrane (CAM) assay. Inhibition of ADORA2B activity resulted in reduced number of developing tumors (Figs. 4a and 4b). Moreover, increasing concentrations of PSB-603 resulted in reduced size of the developing tumors (Figs. 4c and 4d), significant reduction of proliferating Ki67 (MKI67)-positive tumor cells and strong reduction of tumor-induced vascularization of xenografts, demonstrated by staining with the pericyte marker desmin (DES; Figs. 4d–4f).

ADORA2B depletion in HNSCC results in reduced tumor growth *in vitro* and *in vivo*

To validate our inhibitor data presented in Figure 4, knock-down experiments were performed. HNSCC cells were transduced with lentiviruses, expressing either scrambled shRNA (shScr) or shRNA targeting *ADORA2B* (shADORA2B). We confirmed the abrogation of *ADORA2B* expression in UDSCC1 by quantitative RT-PCR (Fig. 5a). Real-time cell analyses revealed a clear dependence of UDSCC1 cells on ADORA2B expression for autonomous cell proliferation (Fig. 5b). To analyze the effect of ADORA2B down-modulation *in vivo*, scrambled or ADORA2B-specific shRNA infected UDSCC1 were xenografted in two different amounts (1.5×10^6 and 2.0×10^6) on the CAM of chicken embryos and tumor development was assessed. Abrogation of ADORA2B expression resulted in markedly reduced tumor formation capability *in vivo* (Figs. 5c and 5d). This was associated with significantly reduced tumor size (Fig. 5e), reduced proliferation index, as well as reduced tumor-induced vascularization (Figs. 5f–5h), independent of the cell number initially seeded. Together, these data strongly suggest that ADORA2B is an important modulator of HNSCC autonomous cell growth *in vitro* and *in vivo* and therefore a potential therapeutic target for HNSCC treatment.

Discussion

The adenosinergic system plays an important role in the development of many types of cancer.[4] To investigate the importance of ADO-generating and sensing molecules in HNSCC, we first studied the presence of these molecules involved in these processes in HNSCC-derived cell lines *in vitro*. Our study shows that ENTPD1 is not expressed in HNSCC-derived cells, neither at mRNA nor at protein level. Since hypoxic conditions are responsible for upregulation of ENTPD1 within the TME,[36] cultivation of cells under normoxic settings could explain this observation. In contrast, a considerable expression of NT5E in HNSCC cells was observed. This finding is in line with previous reports demonstrating significantly higher expression of NT5E in epithelial dysplasia and HNSCC compared to normal oral mucosa.[37] Moreover, NT5E expression in HNSCC was found to be associated with lymph node metastasis and poor prognosis.[37] Contrary to findings of the aforementioned study,[37] we were not able to detect any coexpression of NT5E with ADORA2A or ADORA3. In agreement with the findings of Kasama et al.,[27] we detected exclusively ADORA2B in HNSCC

cells. Kasama and colleagues showed a substantial upregulation of ADORA2B in oral squamous cell carcinoma (OSCC)-derived cell lines as well as in primary OSCC compared to normal oral keratinocytes or normal oral tissue.[27] ADORA2B is one of four ADO sensing receptors exhibiting the lowest ADO affinity.[35] Physiological ADO concentrations below 1.0 μM are not sufficient to activate ADORA2B.[38] Therefore it was suggested, that ADORA2B may play an important role in tumor conditions associated with hypoxia-induced cell death and subsequent ATP release, in which ADO concentrations can reach 50–100 μM inside the TME.[8] The expression of both NT5E and ADORA2B in HNSCC-derived cells suggests the contribution of the adenosinergic system in the development, maintenance and progression of HNSCC. Although ADORA2B was found to be implicated in many types of solid tumors,[21–27] its precise role in HNSCC carcinogenesis is not well understood. Therefore, the present study focused on the identification of the oncogenic function of ADORA2B in HNSCC-derived tumor cells.

We found that treatment with ADO had no effect on HNSCC cell proliferation. Even high concentrations of ADO (10 μM), associated with elevation of intracellular cAMP levels, failed to promote cell proliferation. In line with previous findings,[20,39] ADO concentrations of 10 mM (at least 100-fold higher than in a hypoxic TME[8]) induced apoptosis in analyzed cell lines through an ADORA2B-independent mechanism, possibly mediated by intracellular transport of ADO.[40] Also, the ADORA2B agonist NECA showed only moderate or no influence on ADORA2B activity measured by intracellular cAMP content, wound closure assay, protein expression of cell cycle associated genes and VEGFA secretion. We assume that these observations are caused by the constitutive ADORA2B activity revealed in HNSCC-derived cells, as considerable basal cAMP levels were detected in our study, even in the presence of ADA abolishing the influence of endogenous ADO on ADORA2B activity.

ADORA2B belongs to a large family of GPCR known to possess certain levels of constitutive activity even in the absence of activating mutations.[41–43] Furthermore, elevated levels of intracellular cAMP with increasing expression levels of transfected GPCR were observed.[44] In line with these observations, the upregulation of ADORA2B in HNSCC shown in the present study and by others[27] could be responsible for the constitutive ADORA2B activity observed in HNSCC cells. Moreover, Vecchio et al.[43] reported a ligand-independent ADORA2B activity in native cells derived from prostate cancer. Thus, the fact that similar ADORA2B characteristics are observed in different tumor entities, such as prostate cancer- and HNSCC-derived cells, suggests that constitutive ADORA2B activity might be a general phenomenon among various cancer entities.

In contrast, the ADORA2B antagonist PSB-603 efficiently inhibited proliferation of HNSCC cells in a concentration-dependent manner, which was associated with decreased concentration of intracellular cAMP. Moreover, we showed that PSB-603 induced cell cycle arrest as well as apoptosis. Notably,

Molecular Cancer Biology

in colorectal cancer cells, PSB-603 induces alteration in cell metabolism changing the redox state in an ADORA2B-independent manner.[40] Thus, the observed reduction of Namalwa cell proliferation in the MTT assay under 10 μM PSB-603 may be caused by ROS-mediated induction of apoptosis. Also, we cannot exclude a PSB-603-induced ROS production in HNSCC-derived cells that may further contribute to ADORA2B-independent induction of apoptosis even at lower concentrations. However, shRNA-mediated inhibition of ADORA2B activity in HNSCC cells reduced tumor formation, proliferation and vascularization in in vivo xenograft experiments. Therefore, an A2B-dependent effect on HNSCC tumorigenesis was confirmed, and a PSB-603-induced ADORA2B-dependent effect on tumor growth and vascularization can be concluded.

ADORA2B activates various different signaling pathways depending on the type of G protein subunit, $G\alpha_s$, G_q or $G_{i/o}$ coupling to the receptor.[35,45–50] Similar to PSB-603 treatment, inhibition of the phospholipase C results in the reduction of VEGF secretion and the abrogation of adenylate cyclase activity leads to the inhibition of HNSCC cell proliferation. Therefore, after ligation of ADORA2B, an involvement of G_q- as well as $G_{\alpha s}$-mediated signaling can be suggested. However, the A2B-induced downstream signaling pathways in HNSCC-derived tumor cells remain to be elucidated. In contrast to the present study describing an A2B-mediated protumorigenic effect on HNSCC, activation of ADORA2A (also utilizing $G_{\alpha s}$ and therefore elevated cAMP levels for intracellular signal transduction[46]) induces antitumorigenic effects in colon cancer and hepatoma cells.[13,14] Notably, in melanoma cells ADO-concentration dependent pro-proliferative and antiproliferative effects through ADORA2A activation were observed.[20] A2A-mediated protumorigenic effects were also found in lung and breast cancer cells.[15,16] The opposite effects mediated by ADORA2A and ADORA2B may depend on (i) the basal receptor activation status as we observed a constitutive, ligand-independent ADORA2B activity in HNSCC cells, which was not described for ADORA2A, (ii) the concentration of extracellular ligand, (iii) the ADO-receptor-independent agonist or antagonist action, (iv) the expression of additional ADO-sensing receptors, (v) the ADO-receptor-mediated intracellular signaling cascade, and on (vi) the tumor entity. Thus, further investigation on ADO-receptor function and signaling is needed to better understand their precise role in the development and maintenance of cancer.

Together, our data suggest ADORA2B being an important biomarker and an interesting therapeutic target for treatment of HNSCC as well as other ADORA2B expressing solid tumor entities hitting two important cancer characteristics: cell viability and angiogenesis.

Acknowledgements

Conflict of interest

All authors declare no commercial or financial conflict of interest.

References

1. Global Burden of Disease Cancer Collaboration, Fitzmaurice C, Allen C, et al. Global, regional, and National Cancer Incidence, mortality, years of life lost, years lived with disability, and disability-adjusted life-years for 32 cancer groups, 1990 to 2015 a systematic analysis for the global burden of disease study. JAMA Oncol 2017;3: 524–48.

2. Whiteside TL. Head and neck carcinoma immunotherapy: facts and hopes. Clin Cancer Res 2017; 24:1261.

3. Ferris RL. Immunology and immunotherapy of head and neck cancer. J Clin Oncol 2015;33: 3293–305.

4. Allard B, Beavis PA, Darcy PK, et al. Immunosuppressive activities of adenosine in cancer. Curr Opin Pharmacol 2016;29:7–16.

5. Allard B, Longhi MS, Robson SC, et al. The ectonucleotidases CD39 and CD73: novel checkpoint inhibitor targets. Immunol Rev 2017;276: 121–44.

6. de Mello PA, Coutinho-Silva R, Savio LEB. Multifaceted effects of extracellular adenosine triphosphate and adenosine in the tumor-host interaction and therapeutic perspectives. Front Immunol 2017;8:1–17.

7. Theodoraki MN, Hoffmann TK, Jackson EK, et al. Exosomes in HNSCC plasma as surrogate

markers of tumour progression and immune competence. Clin Exp Immunol 2018;194:67–78.

8. Vaupel P, Mayer A. Hypoxia-driven adenosine accumulation: a crucial microenvironmental factor promoting tumor progression. Adv Exp Med Biol 2016;876:177–83.

9. Fredholm BB, IJzerman AP, Jacobson KA, et al. LXXXI. Nomenclature and classification of adenosine receptors-an update. Pharmacol Rev 2011; 63:1–34.

10. Dastjerdi N, Valiani A, Mardani M, et al. Adenosine A1 receptor modifies P53 expression and apoptosis in breast cancer cell line Mcf-7. Bratisl Med J 2016;117:242–6.

11. Dastjerdi M, Rarani M, Valiani A, et al. The effect of adenosine A1 receptor agonist and antagonist on p53 and caspase 3, 8, and 9 expression and apoptosis rate in MCF-7 breast cancer cell line. Trends Pharmacol Sci 2016;11:303–10.

12. Saito M, Yaguchi T, Yasuda Y, et al. Adenosine suppresses CW2 human colonic cancer growth by inducing apoptosis via A1 adenosine receptors. Cancer Lett 2010;290:211–5.

13. Yasuda Y, Saito M, Yamamura T, et al. Extracellular adenosine induces apoptosis in Caco-2 human colonic cancer cells by activating caspase-9/−3 via A2a adenosine receptors. J Gastroenterol 2009;44: 56–65.

14. Tamura K, Kanno T, Fujita Y, et al. A 2a adenosine receptor mediates HepG2 cell apoptosis by downregulating Bcl-X L expression and upregulating bid expression. J Cell Biochem 2012; 113:1766–75.

15. Mediavilla-Varela M, Luddy K, Noyes D, et al. Antagonism of adenosine A2A receptor expressed by lung adenocarcinoma tumor cells and cancer associated fibroblasts inhibits their growth. Cancer Biol Ther 2013;14:860–8.

16. Gessi S, Bencivenni S, Battistello E, et al. Inhibition of A2A adenosine receptor signaling in cancer cells proliferation by the novel antagonist TP455. Front Pharmacol 2017;8:1–13.

17. Kim S-J, Min H-Y, Chung H-J, et al. Inhibition of cell proliferation through cell cycle arrest and apoptosis by thio-cl-IB-MECA, a novel A3 adenosine receptor agonist, in human lung cancer cells. Cancer Lett 2008;264:309–15.

18. Aghaei M, Panjehpour M, Karami-Tehrani F, et al. Molecular mechanisms of A3 adenosine receptor-induced G1 cell cycle arrest and apoptosis in androgen-dependent and independent prostate cancer cell lines: involvement of intrinsic pathway. J Cancer Res Clin Oncol 2011;137: 1511–23.

19. Kim H, Kang JW, Lee S, et al. A3 adenosine receptor antagonist, truncated thio-cl-IB-MECA,

induces apoptosis in T24 human bladder cancer cells. *Anticancer Res* 2010;30:2823–30.

20. Merighi S, Mirandola P, Milani D, et al. Adenosine receptors as mediators of both cell proliferation and cell death of cultured human melanoma cells. *J Invest Dermatol* 2002;119:923–33.

21. Zhou Y, Chu X, Deng F, et al. The adenosine A2b receptor promotes tumor progression of bladder urothelial carcinoma by enhancing MAPK signaling pathway. *Oncotarget* 2017;8:48755–68.

22. Cekic C, Sag D, Li Y, et al. Adenosine A2B receptor blockade slows growth of bladder and breast tumors. *J Immunol* 2012;188:198–205.

23. Ma DF, Kondo T, Nakazawa T, et al. Hypoxia-inducible adenosine A2B receptor modulates proliferation of colon carcinoma cells. *Hum Pathol* 2010;41:1550–7.

24. Mittal D, Sinha D, Barkauskas D, et al. Adenosine 2B receptor expression on cancer cells promotes metastasis. *Cancer Res* 2016;76:4372–82.

25. Wei Q, Costanzi S, Balasubramanian R, et al. A2B adenosine receptor blockade inhibits growth of prostate cancer cells. *Purinergic Signal* 2013;9:271–80.

26. Desmet CJ, Gallenne T, Prieur A, et al. Identification of a pharmacologically tractable Fra-1/ADORA2B axis promoting breast cancer metastasis. *Proc Natl Acad Sci USA* 2013;110:5139–44.

27. Kasama H, Sakamoto Y, Kasamatsu A, et al. Adenosine A2b receptor promotes progression of human oral cancer. *BMC Cancer* 2015;15:563.

28. Lansford CD, Grenman R, Bier H, et al. *Human cell culture Vol. II: cancer cell lines part 2; chapter 28: head and neck cancers*. London: Kluwer Academic Publishers, 1999. 185–276.

29. Ballo H, Koldovsky P, Hoffmann T, et al. Establishment and characterization of four cell lines derived from human head and neck squamous cell carcinomas for an autologous tumor-fibroblast in vitro model. *Anticancer Res* 1999;19:3827–36.

30. Osswald CD, Xie L, Guan H, et al. Fine-tuning of FOXO3A in cHL as a survival mechanism and a hallmark of abortive plasma cell differentiation. *Blood* 2018;131:1556–67.

31. Livak KJ, Schmittgen TD. Analysis of relative gene expression data using real-time quantitative PCR and the 2-ΔΔCT method. *Methods* 2001;25:402–8.

32. Azoitei N, Diepold K, Brunner C, et al. HSP90 supports tumor growth and angiogenesis through PRKD2 protein stabilization. *Cancer Res* 2014;74:7125–36.

33. Schindelin J, Arganda-Carrera I, Frise E, et al. Fiji—an open platform for biological image analysis. *Nat Methods* 2009;9:676–82.

34. Saze Z, Schuler P, Hong C, et al. Adenosine production by human B cells and B cell–mediated suppression of activated T cells. *Blood* 2013;122:9–19.

35. Vecchio EA, White PJ, May LT. The adenosine A2B G protein-coupled receptor: recent advances and therapeutic implications. *Pharmacol Ther* 2019;198:20–33.

36. Hartfield SM, Kjaergaard J, Lukashev D, et al. Systemic oxygenation weakens the hypoxia and hypoxia inducible factor 1α-dependent and extracellular adenosine-mediated tumor protection. *J Mol Med* 2014;92:1283–92.

37. Ren Z-H, Lin C-Z, Cao W, et al. CD73 is associated with poor prognosis in HNSCC. *Oncotarget* 2016;7:61690–702.

38. Spychala J. Tumor-promoting functions of adenosine. *Pharmacol Ther* 2000;87:161–73.

39. Schrier SM, Van Tilburg EW, Van der Meulen H, et al. Extracellular adenosine-induced apoptosis in mouse neuroblastoma cells studies on involvement of adenosine receptors and adenosine uptake. *Biochem Pharmacol* 2001;61:417–25.

40. Li S, Li X, Guo H, et al. Intracellular ATP concentration contributes to the cytotoxic and Cytoprotective effects of adenosine. *PLoS One* 2013;8:e76731.

41. Samama P, Cotecchia S, Costa T, et al. Mutation-induced activated state of the beta-adrenergic receptor. *J Biol Chem* 1993;268:4625–36.

42. Lefkowitz RJ, Cotecchina S, Samama P, et al. Constitutive activity of receptors coupled to guanine nucleotide regulatory proteins. *Trends Pharmacol Sci* 1993;14:303–7.

43. Vecchio EA, Tan CYR, Gregory KJ, et al. Ligand-independent adenosine A2B receptor constitutive activity as a promoter of prostate cancer cell proliferation. *J Pharmacol Exp Ther* 2016;357:36–44.

44. Costa T, Ogino Y, Munson PJ, et al. Drug efficacy at guanine nucleotide-binding regulatory protein-linked receptors: thermodynamic interpretation of negative antagonism and of receptor activity in the absence of ligand. *Mol Pharmacol* 1992;41:549–60.

45. Feoktistov I, Goldstein AE, Ryzhov S, et al. Differential expression of adenosine receptors in human endothelial cells: role of A2B receptors in angiogenic factor regulation. *Circ Res* 2002;90:531–8.

46. Fredholm BB, IJzerman AP, Jacobson KA, et al. International Union of Pharmacology. XXV. Nomenclature and classification of adenosine receptors. *Pharmacol Rev* 2001;53:527–52.

47. Yang G, Sau C, Lai W, et al. On the G protein-coupling selectivity of the native A2B adenosine receptor. *Biochem Pharmacol* 2018;151:201–13.

48. Fang Y, Olah ME. Cyclic AMP-dependent, protein kinase A-independent activation of extracellular signal-regulated kinase 1 / 2 following adenosine receptor stimulation in human umbilical vein endothelial cells: role of exchange protein activated by cAMP 1 (Epac1). *J Pharmacol Exp Ther* 2007;322:1189–200.

49. Schulte G, Fredholm BB. The GS-coupled adenosine A2Breceptor recruits divergent pathways to regulate ERK1/2 and p38. *Exp Cell Res* 2003;290:168–76.

50. Grant MB, Davis MI, Caballero S, et al. Proliferation, migration, and ERK activation in human retinal endothelial cells through a(2B) adenosine receptor stimulation. *Invest Ophthalmol Vis Sci* 2001;42:2068–73.